

Supporting Information:

Toward Prediction of Nonradiative Decay
Pathways in Organic Compounds I: The Case
of Naphthalene Quantum Yields

Alexander W. Kohn,^{†,‡} Zhou Lin,^{†,‡} and Troy Van Voorhis*,[†]

[†]*Department of Chemistry, Massachusetts Institute of Technology, Cambridge, MA 02139*

[‡]*These authors contributed equally.*

E-mail: tvan@mit.edu

CONTENTS:

1. Table S1: The absorption energy (E_{abs}), the fluorescent energy (E_{fl}), and the radiative rate (k_{fl}) for family I from theory and experiments.
2. Table S2: The absorption energy (E_{abs}), the fluorescent energy (E_{fl}), and the radiative rate (k_{fl}) for family II from theory and experiments.
3. Table S3: The experimental nonradiative rate (k_{nr}) is compared against the theoretical direct intersystem crossing rate (k_{ISC}) for family I. The theoretical values of the adiabatic energy gap (E_{ISC}), the reorganization energy (λ_{ISC}), and the Marcus-defined activation energy ($E_{\text{ISC}}^{\ddagger}$) are also provided.
4. Table S4: The experimental nonradiative rate (k_{nr}) is compared against the theoretical direct internal conversion rate (k_{IC}) for family II. The theoretical values of the fluorescence energy (E_{fl}), the reorganization energy (λ_{IC} , half of the Stokes shift), and the Marcus-defined activation energy (E_{IC}^{\ddagger}) are also provided.
5. Figure S1: Comparison between the theoretical and experimental values for the absorption energy (E_{abs}) for families I and II.
6. Figure S2: Energy gap law correlation between the total non-radiative rate (k_{nr}) and the activation energy (E_{a}) evaluated using the SF-DFT/BHHLYP approach. The activation energy is treated as the difference between the Frank-Condon (FC) minimum on the S_1 surface and the S_1/S_0 minimum energy conical intersection (MECI).
7. Figure S3: The squared transition dipole moments ($|\mu|^2$) of the $S_0 \rightarrow S_1$ and $S_0 \rightarrow S_2$ transitions along the reaction path described in Figure 6 of the main text. S_1 and S_2 do not seem to switch in character.
8. Figure S4: The percentage of the largest natural transition orbital (NTOs) of the $S_0 \rightarrow S_1$ and $S_0 \rightarrow S_2$ transitions along the reaction path described in Figure 6 of the main text. S_1 and S_2 do not seem to switch in character.

Table S1: E_{abs} , E_{fl} , and k_{fl} for family I from theory and experiments.

#	species	E_{abs} (eV)		E_{fl} (eV)		$\log_{10}(k_{\text{fl}}/\text{s}^{-1})$	
		theory	expt ^a	theory	expt ^a	theory ^f	expt ^a
1	NAPH	4.66	4.31	4.27	3.85	7.97	6.38
2	1MN	4.62	4.39	4.18	3.81	8.06	6.57
3	2MN	4.58	4.31	4.17	3.87	7.89	6.73
4	1HN	4.57	4.28	4.03	3.80	7.94	7.30
5	2HN	4.38	4.34	4.01	3.70	7.81	7.38
6	23DMN	4.53	4.28	4.16	3.86	7.85	6.69
7	26DMN	4.52	4.36	4.19	3.80	7.76	7.07
8	2PN	4.36	4.29	3.92	3.55	8.56	6.36
9	14DPN	4.20	4.12	3.37	3.26	8.66	8.33
10	15DPN	4.28	4.10	3.50	3.31	8.56	8.48
11	17DPN	4.20	4.17	3.42	3.40	8.38	7.18
12	ACN	4.58	4.30	4.13	3.86	8.10	7.29
$\langle \Delta_X \rangle^{b,c}$		0.19		0.27		0.98	
$\langle \Delta_X \rangle^{b,d}$		0.19		0.27		0.98	

^a Experimental values are reported by Berlman *et al.*^{S1}

^b $\Delta_X = X_{\text{theory}} - X_{\text{expt}}$. $X = E_{\text{abs}}$, E_{fl} , or k_{fl} .

^c Mean signed error (MSE).

^d Mean absolute error (MAE).

^f Kasha emission $S_1 \rightarrow S_0$.

Table S2: E_{abs} , E_{fl} , and k_{fl} for family II from theory and experiments.

#	species	E_{abs} (eV)		E_{fl} (eV)		$\log_{10}(k_{\text{fl}}/\text{s}^{-1})$	
		theory	expt	theory	expt	theory ^g	expt
13	1AN ^a	4.25	3.90	3.60	3.29	7.82	7.82
14	1A4CNN ^a	4.18	3.72	3.74	3.22	8.17	8.15
15	1A4CLN ^a	4.12	3.79	3.48	3.19	7.88	7.88
16	1A4MN ^a	4.14	3.82	3.44	3.18	7.82	7.72
17	1MAN ^a	4.14	3.72	3.52	3.23	7.87	7.80
18	1DMAN ^b	4.18	4.07	3.54	3.22	7.97	7.93
19	1DMA4CNN ^a	4.00	3.69	3.57 ^h	3.17	8.27 ^h	8.54
20	1DMA4CLN ^a	4.06	3.89	3.44	3.14	8.03	8.03
21	1DMA4MN ^a	4.11	3.96	3.42	3.14	7.95	7.92
22	1DMA4MON ^b	4.06	3.77	3.23	3.01	7.82	7.90
23	1DMA5MON ^b	4.28	4.08	3.73	3.35	8.22	7.90
24	1DMA6MON ^b	4.11	4.09	3.50	3.22	7.95	7.86
25	1DMA7MON ^b	4.04	4.22	3.42	3.15	7.92	7.70
26	1NAZN ^c	4.15	3.80	3.55	3.17	7.99	7.89
27	1NPYN ^c	4.06	3.90	3.54 ^h	3.21	8.01 ^h	7.94
	$\langle \Delta_X \rangle^{d,e}$	0.23		0.32		0.05	
	$\langle \Delta_X \rangle^{d,f}$	0.26		0.32		0.05	

^a Experimental values are reported by Suzuki *et al.*^{S2}

^b Experimental values are reported by Takehira *et al.*^{S3}

^c Experimental values are reported by Rückert *et al.*^{S4}

^d $\Delta_X = X_{\text{theory}} - X_{\text{expt}}$. $X = E_{\text{abs}}$, E_{fl} , or k_{fl} .

^e Mean signed error (MSE).

^f Mean absolute error (MAE).

^g Kasha emission $S_1 \rightarrow S_0$.

^h These values are evaluated at an S_1 geometry optimized using a range-separated variant of PBE with 50% Hartree–Fock exchange in the short-range and $\omega = 0.2 \text{ bohr}^{-1}$ as the species collapsing into an unphysical charge-transfer excited state.

Table S3: The experimental k_{nr} is compared against the theoretical direct k_{ISC} for family I. The theoretical values of E_{ISC} , λ_{ISC} , and $E_{\text{ISC}}^{\ddagger}$ are also provided.

#	Species	$\log_{10}(k_{\text{nr}}/\text{s}^{-1})^a$	$\log_{10}(k_{\text{ISC}}/\text{s}^{-1})^b$	E_{ISC} (eV)	λ_{ISC} (eV)	$E_{\text{ISC}}^{\ddagger}$ (eV)
		expt ^a	theory	theory	theory	theory
1	NAPH	6.90	6.92	1.41	0.26	2.71
2	1MN	7.05	7.08	1.36	0.25	2.58
3	2MN	7.06	7.36	1.39	0.26	2.63
4	1HN	7.87	7.43	1.26	0.25	2.30
5	2HN	7.71	7.86	1.29	0.26	2.32
6	23DMN	6.90	7.65	1.37	0.25	2.60
7	26DMN	7.16	7.62	1.35	0.24	2.63
8	2PN	6.81	7.12	1.17	0.29	1.83
9	14DPN	8.51	7.96	1.00	0.30	1.41
10	15DPN	8.42	7.74	1.02	0.25	1.61
11	17DPN	7.23	7.07	0.98	0.26	1.46
12	CAN	7.12	6.92	1.31	0.25	2.42

^a Experimental values are reported by Berlman *et al.*^{S1}

^b Theoretical values in this work are predicted using Equation 5 in the main text with $B = 8.32 \times 10^6 \text{ s}^{-1}$ and $C = 1.66 \times 10^7 \text{ s}^{-1} \text{ cm}^2$, respectively.

Table S4: The experimental k_{nr} is compared against the theoretical direct k_{IC} for family II. The theoretical values of E_{fl} , λ_{IC} , and E_{IC}^{\ddagger} are also provided.

#	Species	$\log_{10}(k_{\text{IC}}/\text{s}^{-1})^{a,b,c}$	$\log_{10}(k_{\text{IC}}/\text{s}^{-1})^d$	E_{IC}^e (eV)	λ_{IC} (eV)	E_{IC}^{\ddagger} (eV)
		expt	theory	theory	theory	theory
13	1AN ^a	7.92	7.39	3.61	0.37	10.80
14	1A4CNN ^a	9.21	9.07	3.46	0.26	13.20
15	1A4CLN ^a	8.25	7.54	3.47	0.36	10.21
16	1A4MN ^a	7.49	6.52	3.49	0.38	9.81
17	1MAN ^a	7.66	7.76	3.55	0.35	10.87
18	1DMAN ^b	9.93	9.13	3.59	0.40	9.97
19	1DMA4CNN ^a	11.24	10.92	3.34	0.29	11.31
20	1DMA4CLN ^a	10.24	9.39	3.46	0.39	9.53
21	1DMA4MN ^a	9.36	8.73	3.51	0.42	9.24
22	1DMA4MON ^b	8.45	8.36	3.44	0.46	8.34
23	1DMA5MON ^b	9.85	9.31	3.66	0.34	11.85
24	1DMA6MON ^b	9.85	8.26	3.49	0.37	10.16
25	1DMA7MON ^b	7.91	-	3.45	0.37	9.84
26	1NAZN ^c	8.68	9.72	3.52	0.36	10.56
27	1NPYN ^c	10.09	11.29	3.50	0.32	11.52

^a Experimental values are reported by Suzuki *et al.*^{S2}

^b Experimental values are reported by Takehira *et al.*^{S3}

^c Experimental values are reported by Rückert *et al.*^{S4}

^d Theoretical values in this work are predicted using Equation 5 in the main text with $A_{\text{IC}} = 2.02 \times 10^{12} \text{ s}^{-1}$ and a slope of -8.18 eV^{-1} .

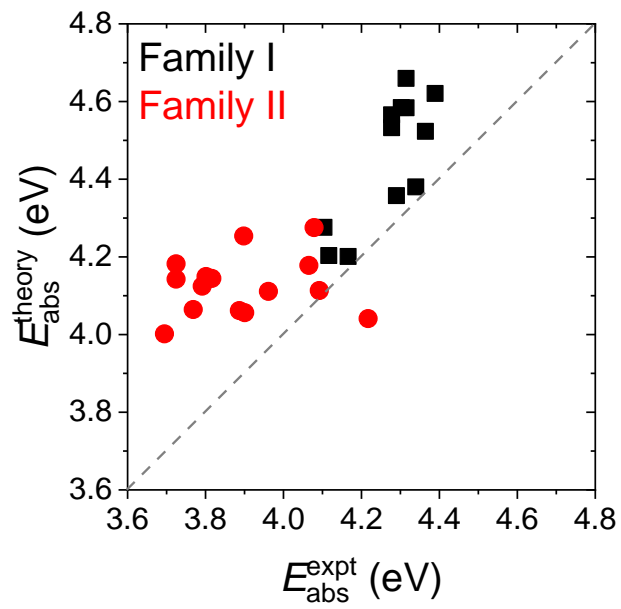


Figure S1: Comparison between the theoretical and experimental values for E_{abs} for families I (black squares) and II (red circles).

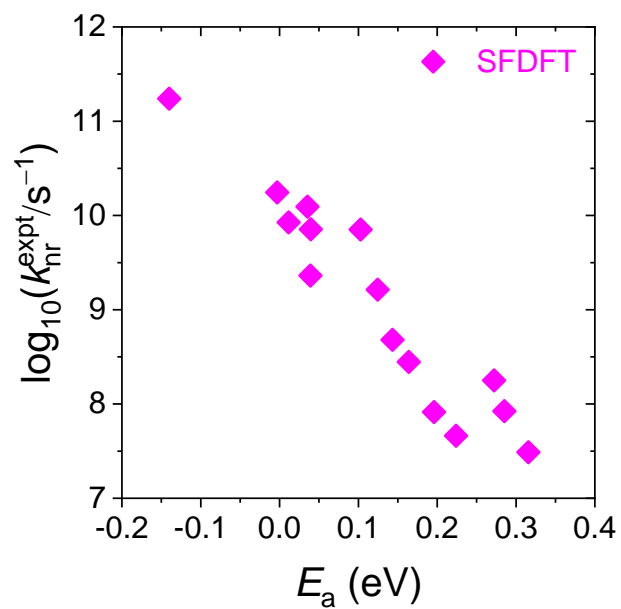


Figure S2: Energy gap law correlation between k_{nr} and E_a evaluated using the SFDFT/BHHLYP approach. E_a is treated as the difference between the FC minimum on the S_1 surface and the S_1/S_0 MECI.

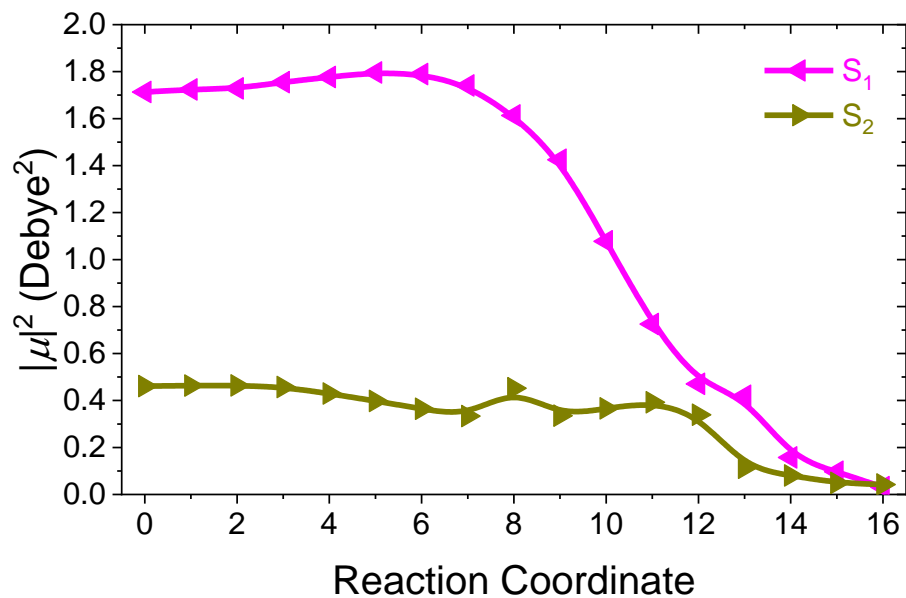


Figure S3: $|\mu|^2$'s of the $S_0 \rightarrow S_1$ and $S_0 \rightarrow S_2$ transitions along the reaction path described in Figure 6 of the main text. S_1 and S_2 do not seem to switch in character.

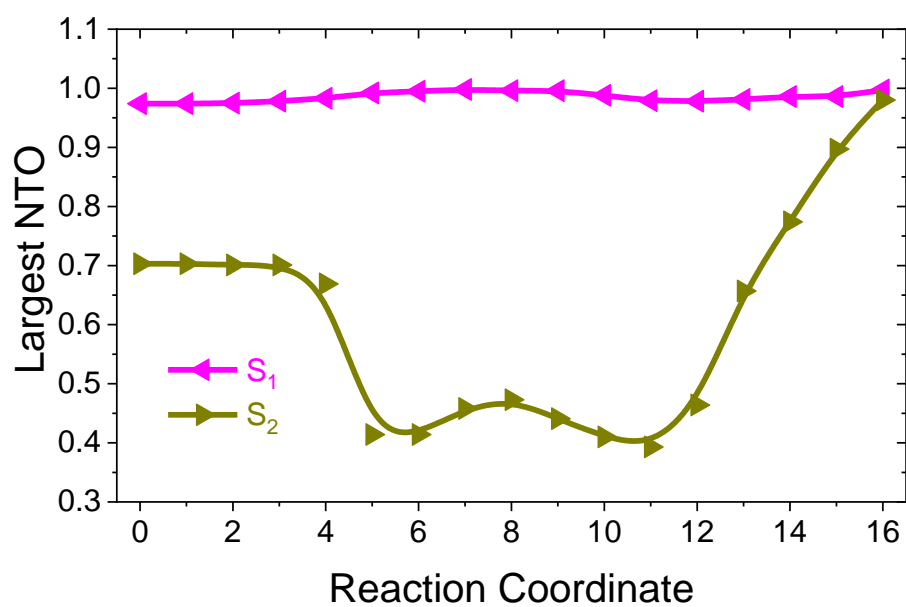


Figure S4: The percentage of the largest NTOs of the $S_0 \rightarrow S_1$ and $S_0 \rightarrow S_2$ transitions along the reaction path described in Figure 6 of the main text. S_1 and S_2 do not seem to switch in character.

References

- (S1) Berlman, I. B. In *Handbook of Fluorescence Spectra of Aromatic Molecules*, 2nd ed.; Berlman, I. B., Ed.; Academic Press, 1971; pp 107–415.
- (S2) Suzuki, K.; Demeter, A.; Kühnle, W.; Tauer, E.; Zachariasse, K. A.; Tobita, S.; Shizuka, H. Internal conversion in 4-substituted 1-naphthylamines. Influence of the electron donor/acceptor substituent character. *Phys. Chem. Chem. Phys.* **2000**, *2*, 981–991.
- (S3) Takehira, K.; Suzuki, K.; Hiratsuka, H.; Tobita, S. Fast internal conversion in 1-(dimethylamino)naphthalene: Effects of methoxy substitution on the naphthalene ring. *Chem. Phys. Lett.* **2005**, *413*, 52–58.
- (S4) Rückert, I.; Demeter, A.; Morawski, O.; Kühnle, W.; Tauer, E.; Zachariasse, K. A. Internal conversion in 1-aminonaphthalenes. Influence of amino twist angle. *J. Phys. Chem. A* **1999**, *103*, 1958–1966.